Giant *Centella asiatica*, a novel cultivar rich in madecassoside and asiaticoside, suppresses α-melanocyte-stimulating hormone-induced melanogenesis through MC1R binding

JIWON SEO[1*], CHANHYEOK JEONG[1*], SEUNG MAN OH[1], SUNG-YOUNG LEE[2], HAN WOONG PARK[3], DAE BANG SEO[3], DAE SUNG YOO[3], WOO-JIN SIM[4], TAE-GYU LIM[4,5], JUNG HAN YOON PARK[2], CHANG HYUNG LEE[2,6] and KI WON LEE[1,2,7-9]

[1]Department of Agricultural Biotechnology and Research Institute of Agriculture and Life Sciences, Seoul National University, Seoul 08826, Republic of Korea; [2]Bio-MAX Institute, Seoul National University, Seoul 08826, Republic of Korea; [3]ASK Company Co., Ltd., Daegu 42176, Republic of Korea; [4]Department of Food Science and Biotechnology, Sejong University, Seoul 05006, Republic of Korea; [5]Department of Food Science and Biotechnology, and Carbohydrate Bioproduct Research Center, Sejong University, Seoul 05006, Republic of Korea; [6]School of Pharmacy, Sungkyunkwan University, Suwon 16419, Republic of Korea; [7]Advanced Institutes of Convergence Technology, Seoul National University, Suwon 16229, Republic of Korea; [8]Institutes of Green Bio Science and Technology, Seoul National University, Pyeongchang 25354, Republic of Korea; [9]Department of Agricultural Biotechnology and Center for Food and Bio Convergence, Seoul National University, Seoul 08826, Republic of Korea

Received July 19, 2024; Accepted October 18, 2024

DOI: 10.3892/ijmm.2024.5454

Abstract. The present study investigated the anti-melanogenesis effects of Giant *Centella asiatica* (GCA), a new cultivator of *Centella asiatica* (CA) cataloged by the Korea Forest Service in 2022, and compared its efficacy with that of traditional CA. GCA has a high yield per unit area and enhanced antioxidant properties. The anti-melanogenic effects of GCA were investigated using B16F10 melanoma cells and a 3D human skin-equivalent model. Key molecular mechanisms were elucidated through western blotting, cAMP assays and molecular docking studies. Focus was addressed on the effect of GCA on skin whitening by comparing the ability of a GCA extract to inhibit melanin production in B16F10 melanoma cells and a 3D human skin-equivalent model to that of CA. The results showed that the GCA extracts more effectively reduced melanin production, which was attributed to their higher content of two active components, madecassoside and asiaticoside. Further investigation revealed that GCA primarily inhibited melanogenesis through the PKA-cAMP response element-binding (CREB)-microphthalmia-associated transcription factor (MITF) axis, a key regulatory pathway in melanin synthesis. Notably, the present study, to the best of our knowledge, is the first to demonstrate that madecassoside and asiaticoside, the two principal compounds in GCA, directly bound to MC1R, which contributed to the significant skin-whitening effects. Moreover, GCA reduced melanin production in a 3D human skin-equivalent model, showing efficacy within a complex skin environment. These results demonstrated the superior effectiveness of GCA to that of CA for skin anti-melanogenesis, indicating its potential as a promising natural material for targeting pigmentation disorders.

Correspondence to: Dr Chang Hyung Lee, School of Pharmacy, Sungkyunkwan University, 2066 Seobu, Jangan, Suwon 16419, Republic of Korea
E-mail: changhyung@skku.edu

Dr Ki Won Lee, Department of Agricultural Biotechnology and Research Institute of Agriculture and Life Sciences, Seoul National University, 1 Gwanak, Gwanak, Seoul 08826, Republic of Korea
E-mail: kiwon@snu.ac.kr

*Contributed equally

Key words: giant *Centella asiatica*, *Centella asiatica*, anti-melanogenesis, α-MSH, melanocytes, 3D human skin-equivalent model

Introduction

Melanogenesis is the production of melanin pigments by melanocytes in the epidermis and is a natural process that determines skin color and provides protection against ultraviolet (UV) radiation (1-3). When exposed to UVB radiation, keratinocytes in the skin secrete α-melanocyte-stimulating hormone (α-MSH) (4,5), which binds to the melanocortin 1 receptor (MC1R) on melanocytes, leading to intracellular cAMP production (6,7). Elevation of intracellular cAMP levels stimulates transcriptional factors, such as microphthalmia-associated transcription factor (MITF) (8,9) and cAMP response element-binding protein (CREB) through the cAMP-dependent protein kinase (PKA) (9-12). MITF is a transcription factor that binds to the promoter region of tyrosinase in melanogenic genes and upregulates their expression.

Tyrosinase is a key enzyme that has a crucial role in regulating melanin synthesis (13,14). Inhibitors targeting tyrosinase can modulate melanin production, and its expression and activity have significant roles in regulating pigmentation levels (15). This mechanism is part of the skin's natural defense system, aiming to protect the skin from UV radiation by enhancing melanin production in response to UVB exposure (16,17). Although production of melanin is a natural and protective response to UVB exposure, excessive or uneven melanin production can cause various effects, such as hyperpigmentation, dark spots, and an uneven skin tone. Hyperpigmentation may be a symptom of underlying skin conditions, such as melasma or post-inflammatory hyperpigmentation. Specific phytochemicals have been shown to modulate the melanogenesis process, which offers a potential way to mitigate these effects. By targeting key enzymes and signaling pathways involved in melanin synthesis, these agents can help reduce the appearance of hyperpigmentation and promote a more even skin tone. Thus, increased understanding of the intricate molecular mechanisms of how these agents modulate melanogenesis is essential for comprehending melanin's role in skin coloration and its overproduction, which can lead to such hyperpigmentation disorders.

Among the various sources of herbal plants, *Centella asiatica* (CA) has gained significant attention for its potential benefits for skin health. CA is a tropical medicinal plant belonging to the Apiaceae family that thrives in warm and humid climates and is primarily found in Asia, India, Madagascar, China, Malaysia and Indonesia (18). A myth says that tigers would roll around in CA to heal their wounds when injured, leading to the plant being called '*Tiger grass*' (19). CA is a common medicinal herb with a rich history in traditional medicine and has recently gained attention for its potential effects on skin health. Previous research trends in CA include improvements in skin health and in antioxidant, anti-aging, anti-inflammatory and pharmacological effects as well as integration with nanotechnology (19-21). CA's diverse applications in skin care, aging, and other industries underscore its growing significance and the expanding research interest in its benefits for overall well-being since it has been widely used in traditional medicine and cosmetics for its various skin benefits, including wound healing, anti-aging and skin-whitening effects (22-24). These properties are mainly attributed to the presence of triterpenoids, such as madecassoside and asiaticoside, which are typically extracted into organic solvents. Giant CA (GCA), recently registered by the Korea Forest Service (2022), was developed to increase the content of the active ingredients in CA, enhance its size, and improve its resistance to environmental stresses, such as temperature changes and pests. Our previous study (Seo *et al*, unpublished data) found that a water extract of GCA showed potential results in modulating skin troubles. Additionally, GCA has been found to possess antioxidant abilities superior to those of CA. These findings prompted us to investigate the potential skin-whitening effects of a GCA water extract and compare it with those of the traditional CA.

The present study aimed to investigate the superior skin-whitening properties of GCA relative to those of CA and elucidate the underlying mechanisms of action. A comprehensive screening of the anti-melanogenic efficacy of the GCA and CA extracts was conducted, followed by an in-depth comparison of their effects in both B16F10 melanoma cells and 3D human skin-equivalent models. It was also intended to explore the molecular mechanisms behind GCA's skin-whitening effects, focusing on key signaling pathways and regulatory targets involved in melanogenesis. By elucidating the specific molecular targets of GCA, it was aimed to provide a strong foundation for its potential industrial applications in the cosmetic and pharmaceutical sectors.

Materials and methods

Plant materials and extraction methods. GCA and CA dried leaves were cultivated under identical conditions for the same duration as previously described (25) and preserved at -40˚C under regulated conditions. These dried samples were chopped into tiny pieces that were pulverized into a fine powder with an RT-34 mixer from Rong Tsong Precision Technology. The powder was then filtered through a ~20-mesh sieve. To perform the extraction, 300 mg of the powdered GCA and CA samples were immersed in 30 ml of distilled water at 60˚C for 30 min. Following extraction, the solution was centrifuged at 3,000 x g for 10 min at room temperature, filtered through Whatman™ filter paper No. 4 (Cytiva), and then freeze dried.

Reagents. Dulbecco's modified eagle medium was purchased from Hyclone; Cytiva. A solution of penicillin and streptomycin was purchased from CellGro by Mediatech (http://www.cellgro.com). Fetal bovine serum was purchased from Seradigm (https://us.vwr.com/cms/avantor_seradigm). The antibody against tyrosinase (cat. no. AB170905) was obtained from Abcam. Antibodies against MITF (cat. no. AB59201), phospho-PKA (p-PKA; cat. no. 4781S), PKA (cat. no. 4782S), p-CREB (cat. no. 9198S) and CREB (cat. no. 9197S) were purchased from Cell Signaling Technology, Inc. The antibody against β-actin (cat. no. SC-8432) was obtained from Santa Cruz Biotechnology, Inc. A protein assay reagent kit was purchased from Bio-Rad Laboratories, Inc. Arbutin was purchased from MilliporeSigma and dissolved in dimethyl sulfoxide.

Measurement of melanin content. Murine melanoma B16F10 cells were obtained from the Korean Cell Line Bank (Seoul, Republic of Korea). B16F10 cells were seeded at a density of $2x10^5$ cells per 60 mm^2 dish. After overnight incubation at 37˚C, the cells were pretreated with GCA and CA (25-100 μg/ml) for 1 h. Then, 200 nM of α-MSH was added, and the cells were incubated for 72 h. The conditioned media containing extracellular melanin was collected and centrifuged at 13,572 x g for 10 min. Then, the supernatant was transferred to a 96-well plate, and an Epoch microplate reader from BioTek Instruments was used to measure the absorbance at 490 nm (1).

A three-dimensional melanoma cell culture system. The forced-floating method was used to establish a three-dimensional melanoma cell-culture system. In the present study, $1x10^4$ B16F10 cells were cultured in an ultra-low attachment (ULA) 96-well round plate (SPL Life Sciences) at 37˚C. The next day, the cells were co-treated with 200 nM α-MSH,

GCA (25-100 μg/ml), or arbutin (100 μg/ml). The ULA plate was incubated for 3 days at 37˚C. The melanin content in the 3D cell cultures was analyzed by measuring the absorbance at 490 nm (1).

Quantification of the cAMP level. To measure the intracellular cAMP concentration, the cAMP assay was performed with cell lysate using a cAMP assay kit (R&D Systems, Inc.) in accordance with the manufacturer's protocol. B16F10 cells ($2x10^5$ cells per 60 mm^2 dish) were incubated with the indicated concentration of GCA (25-100 μg/ml) and α-MSH for 15 min. Lysates were centrifuged 13,572 x g at 4˚C, and then lysate was used directly. The concentration of cAMP was observed by measuring the absorbance at 450 nm in a plate reader.

Mushroom tyrosinase inhibition assay. To determine the tyrosinase inhibitory effect, 3,4-dihydroxy-L-phenylalanine (L-DOPA) was used as a substrate. To assay the tyrosinase inhibition of GCA, 80 μl of distilled water or 80 μl of L-DOPA, 80 μl of mushroom tyrosinase (27.8 U/ml) and various concentrations of GCA (25-100 μg/ml) were added to each well of a 24-well plate. Arbutin (100 μg/ml) was used as a positive control. The sample was mixed with tyrosinase and a 1 mM L-DOPA substrate to react at 37˚C for 30 min. Tyrosinase activity was measured at 475 nm (2).

Western blot analysis. Cells were lysed in a RIPA lysis solution that included 10 mM Tris (Ph 7.5), 150 mM NaCl, 5 mM EDTA, 0.1% Triton X-100, 1 mM DTT, 0.1 mM PMSF, 10% glycerol, and a protease inhibitor cocktail tablet from GenDEPOT, LLC. BCA protein assay kits were used to quantify protein concentrations in the lysates following the manufacturer's protocol. For protein separation, 10 μg of protein samples underwent electrophoresis in a 10% sodium dodecyl sulfate-polyacrylamide gel electrophoresis system and were then transferred to PVDF membranes supplied by MilliporeSigma. Blocking of the membranes was achieved with 5% skim milk for 1 h at room temperature, followed by overnight incubation at 4˚C with the designated primary antibody (1:1,000 dilution). After attaching the horseradish peroxidase-conjugated with goat anti-mouse IgG secondary antibody (cat. no. 1721019) or goat anti-rabbit IgG (cat. no. 1721019) secondary antibody (both from Bio-Rad Laboratories, Inc.) at a 1:5,000 dilution for 1 h at room temperature, an E-9150 Ez-Capture II device by Atto Corporation was used to detect protein bands (26). The ImageJ software version 1.53k (National Institutes of Health) was used to measure the relative density.

Analytical experimental procedures. GCA and CA extracts were applied in a Thermo Vanquish HPLC system (Thermo Fisher Scientific Inc.) to identify the phytochemicals. An HPLC Cortecs C18 column (2.1x50 mm, 1.6 μm) from Waters Corporation was used to perform the chromatographic separations of the metabolites. The flow rate was set to 0.3 ml/min. A 1-μl aliquot of a 1,000-ppm GCA and CA extract was injected, and the column oven was set to 45˚C. The mobile phases were 0.1% formic acid in HPLC-grade water (Solvent A) and 0.1% formic acid in HPLC-grade acetonitrile (Solvent B). Gradient elution was achieved by running the following gradient program: 0-0.5 min, 5% B; 0.5-3.5 min, 5-100% B; 3.5-4 min, 100% B; 4-4.1 min, 5% B; and a 2-min hold time followed by a 3-min re-equilibration to the starting conditions. High-resolution mass spectrometry (MS) data were obtained on a Thermo TSQ Altis high-resolution mass spectrometer equipped with a hybrid quadrupole-Orbitrap mass analyzer. Electrospray ionization (H-ESI) in positive-ion mode was used to acquire all MS data. The optimized MS parameters were as follows: Spray voltage maintained statically at 3,500 V, sheath gas flow rate set at 50 arbitrary units, auxiliary gas at 10 arbitrary units, and sweep gas at 1 arbitrary unit. The ion-transfer tube and vaporizer temperatures were maintained at 325˚C and 350˚C, respectively. Selected Reaction Monitoring was conducted in positive-ion mode with a cycle time of 0.5 sec. The resolutions of quadrupole 1 (Q1) and quadrupole 3 (Q3) were set to 0.7 and 1.2 full-width at half height, respectively, without the use of a calibrated RF lens. Collision-induced dissociation was performed with a gas pressure of 1.5 mTorr.

Molecular modeling and docking simulation. Molecular docking simulations were conducted to investigate the binding affinity and potential interactions between the melanocortin-1 receptor (MC1R) and selected ligands. The 3D structure of MC1R (PDB ID: 7F4D, α-MSH-bound melanocortin-1 receptor) was obtained from the Protein Data Bank (https://www.rcsb.org/), and the 3D structures of the ligands were sourced from the Drug Bank. Autodock Vina in the AMdock platform (27) was used to conduct docking simulations between MC1R and four selected ligands. A previous study identified α-MSH binding sites at GLU94 and LEU106 on MC1R (28); therefore, a search space of 60 cubic Angstroms was centered on these sites. AMdock generated simulations for the 10 most probable binding configurations from which the results with the lowest energy were selected. The two compounds were further analyzed using the MolDock software (version 7.0.0, http://molexus.io/) to calculate their MolDock scores. The same grid box parameters were applied, and the MolDock optimizer algorithm was used to generate the scores (29).

In vitro pull-down assay and competition assay of α-MSH with madecassoside/asiaticoside. B16F10 cellular supernatant (500 μg) was incubated at 4˚C with asiaticoside-Sepharose 4B beads, madecassoside-Sepharose 4B beads (or Sepharose 4B alone as a control) (100 μl, 50% slurry) in reaction buffer [50 mM Tris (pH 7.5), 5 mM EDTA, 150 mM NaCl, 1 mM DTT, 0.01% Nonidet P-40, 2 μg/ml bovine serum albumin, 0.02 mM PMSF and 1X protease inhibitor mixture] for 24 h at 4˚C. For competition assays, α-MSH (0.2, 2, 20, or 200 μM) was added to the reaction mixture to a final volume of 500 μl and incubated at 4˚C for an additional 24 h. After incubation, the beads were washed five times with buffer [50 mM Tris (pH 7.5), 5 mM EDTA, 150 mM NaCl, 1 mM DTT, 0.01% Nonidet P-40 and 0.02 mM PMSF]. The proteins bound to the beads were then analyzed by immunoblotting.

3D human skin equivalent model. The 3D human skin-equivalent model, Neoderm®-ME from Tego Science, Inc., consists of human epidermal keratinocytes and human melanocytes.

Neoderm®-ME was transferred to a 12-well plate in a maintenance medium (Tego Science, Inc.) containing GCA or arbutin and incubated at 37˚C in 5% CO_2 for 7 days. The medium was changed once every 2 days. On day 7, skin pigmentation was observed by viewing with an Olympus AX70 light microscope (Olympus Corporation). Lysate was collected and subsequently centrifuged at 4˚C for 10 min at 13,572 x g. BCA assay reagent kits were used to measure the protein concentration of the lysate following the manufacturer's protocol to analyze tyrosinase expression.

Fontana-Masson staining. 3D human skin-equivalent samples were fixed overnight in 4% formaldehyde at room temperature, embedded in paraffin, and then cut into 3-μm-thick sections with a microtome. The slides were treated with an ammoniacal silver solution at 56˚C for 30 min, followed by rinsing in distilled water. The slides were then incubated in a 0.2% gold chloride solution at room temperature for 30 sec and then in a 5% sodium thiosulfate solution for 2 min. The sections were incubated in nuclear fast red solution for 5 min and dehydrated three times by use of fresh absolute alcohol. An AX70 light microscope (Olympus Corporation) was used to examine the staining results.

Statistical analyses. Statistical analyses were performed using the SPSS-WIN 12.0K program (SPSS, Inc.). All data are presented as the mean ± standard deviation or standard error of the mean. Unpaired Student's t-test was used for single statistical comparisons and one-way ANOVA followed by Tukey's Honest Significant Difference (HSD) test for multiple comparisons. Differences were considered statistically significant for values of $P<0.05$.

Results

The GCA extract shows superior inhibition of α-MSH-induced melanin secretion in both 2D and 3D models. Research on B16F10 cells has shown that α-MSH increases melanin expression through various pathways (30,31). The concentration of α-MSH and treatment time used in the present study were selected on the basis of previous research results (32,33). It was found that α-MSH effectively induced melanin expression up to 2.4-fold relative to the control. Arbutin was used as a positive control (34,35). Melanin secretion was inhibited more effectively by the GCA extract than by the CA extract (Fig. 1A). Especially at a concentration of 100 μg/ml, the GCA extract exhibited superior efficacy in skin-whitening improvement, with a 77% reduction relative to that of α-MSH induction, whereas the CA extract showed a 45% reduction. To further confirm the anti-melanogenic effect of GCA, a 3D cell-culture model was used, which more closely mimics the *in vivo* skin environment (1). The 3D model visually demonstrated the skin-whitening effect of the GCA extract (Fig. 1B). Quantitative analysis of the melanin content in the 3D model revealed that the GCA extract reduced melanin production dose-dependently, with the 100 μg/ml concentration demonstrated efficacy comparable to that of arbutin (Fig. 1C). These results consistently demonstrated the superior melanin-inhibiting effects of the GCA extract in both 2D and 3D cell-culture systems.

The GCA extract inhibits melanogenesis by modulating the cAMP-PKA-CREB-MITF signaling axis and tyrosinase activity. These results suggested that GCA extract effectively inhibits the PKA-CREB-MITF signaling cascade, which is critical for melanin synthesis. In B16F10 cells, α-MSH significantly elevates cAMP levels, triggering enhanced melanin synthesis (36). This increase in cAMP activates PKA, phosphorylating critical proteins in the melanogenesis pathway (9). The present results showed that α-MSH treatment significantly increased intracellular cAMP levels, which in turn activated PKA. In the presence of GCA extract, a dose-dependent reduction in cAMP levels was observed, suggesting that GCA modulates this signaling cascade by inhibiting the α-MSH-induced cAMP increase (Fig. 2A). To further investigate the effects observed in cells, additional experiments with L-DOPA were performed to determine how the GCA extract affects tyrosinase activity. The experiment targeted tyrosinase extracted from mushrooms and evaluated the inhibitory effect of an GCA extract at various concentrations. By using L-DOPA as a substrate to measure the activity of tyrosinase, it was possible to gain a deeper understanding of how the GCA extract regulates its enzyme's activity, which is crucial in the melanin production process (2,37). Particularly at concentrations of 50 μg/ml and 100 μg/ml (Fig. 2B), the GCA extract exhibited pronounced effects in inhibiting tyrosinase activity. The inhibitory effect of the GCA extract at 100 μg/ml was comparable to that of arbutin, a known tyrosinase inhibitor, indicating that the GCA extract effectively modulated the activity of enzymes critical for melanin production. Tyrosinase is crucial for melanin production, and its activity is regulated by various factors and signaling pathways, including the MC1R-cAMP-PKA-CREB-MITF axis (28,38). The current investigation focused on assessing GCA extract's potential to modulate this pathway and its downstream effects on melanogenesis. Treatment of B16F10 melanoma cells with GCA extract resulted in a dose-dependent decrease in the phosphorylation of PKA and CREB, as well as reduced expression levels of MITF and tyrosinase (Fig. 2C).

Comparative analysis of triterpenoid content in GCA and CA extracts. To identify the key components contributing to the melanin inhibition effect of GCA extract, HPLC-MS/MS analysis of the major triterpenoids was performed in both the GCA and CA extracts. The molecular structures of the four main triterpenoids (madecassoside, asiaticoside, madecassic acid and asiatic acid) are presented in Fig. 3A. Quantitative analysis revealed significant differences in the triterpenoid composition between the GCA and CA extracts (Fig. 3B). Notably, the GCA extract contained substantially higher levels of madecassoside (10.43±0.05 mg/g) than those in the CA extract (2.53±0.01 mg/g). Similarly, asiaticoside content was higher in the GCA extract (1.65±0.01 mg/g) than in the CA extract (0.95±0.01 mg/g). These compounds have been previously reported to possess anti-melanogenic properties (39,40). Interestingly, the levels of madecassic acid and asiatic acid were lower in the GCA extract than in the CA extract. This differential composition suggests that the enhanced melanogenesis inhibitory effect of the GCA extract is primarily attributed to its higher content of madecassoside and

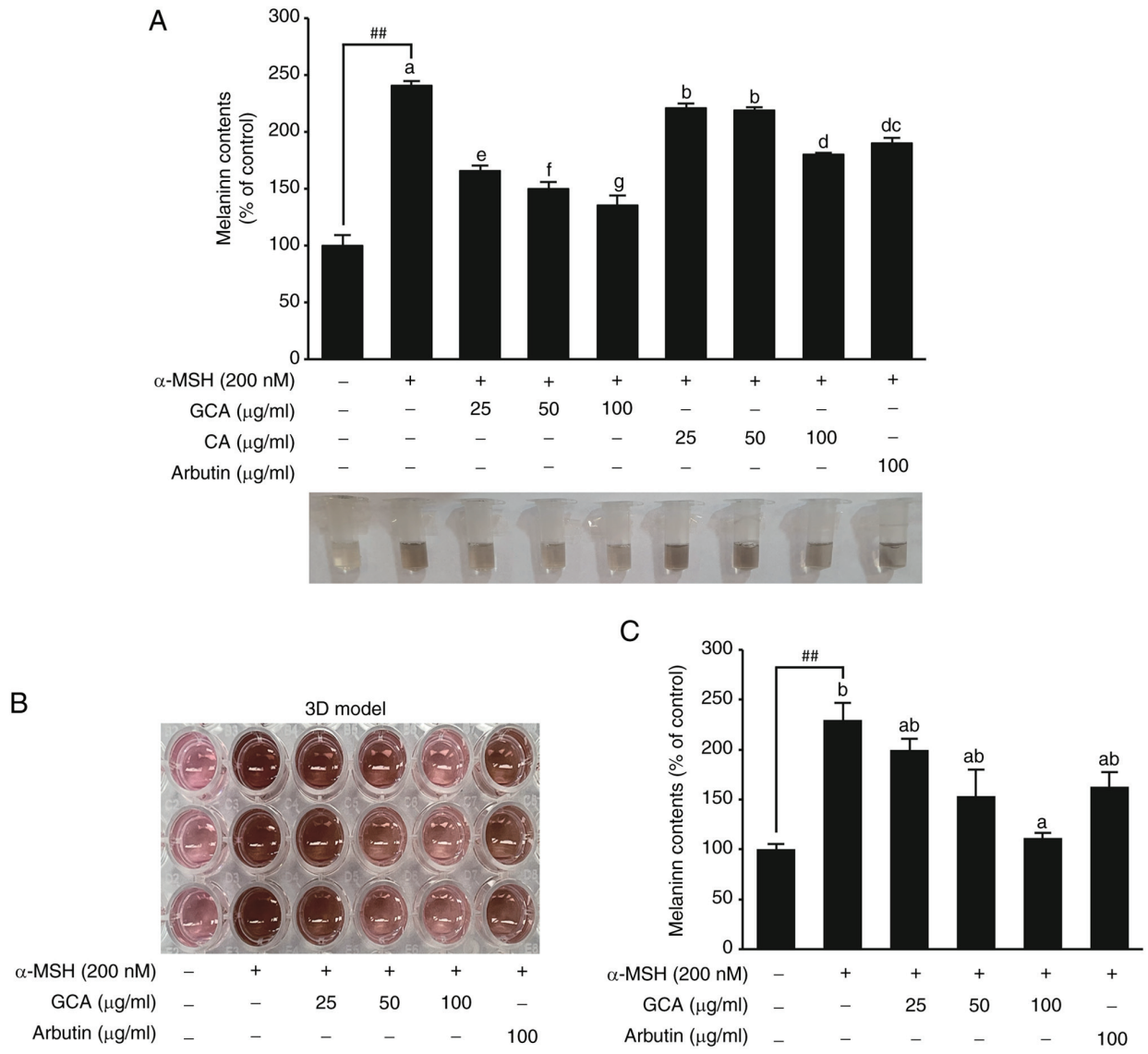

Figure 1. Comparative melanin inhibition by the GCA extract in 2D and 3D models. (A) Effects of the GCA extract and CA extract on the α-MSH-induced extracellular melanin level in the culture media of B16F10 cells. (B) Visual representation of the skin-whitening effect in a 3D human skin-equivalent model. (C) Quantitative analysis of melanin content in the 3D model treated with different concentrations of the GCA extract and arbutin. Data are presented as the mean ± SD (n=3). Significant differences between untreated control and α-MSH-induced group ($^{##}$P<0.01). Mean values with different letters indicate statistically significant differences among the treatment groups, including the α-MSH-induced group, as determined by one-way ANOVA followed by Tukey's Honest Significant Difference (HSD) test (P<0.05). α-MSH, α-melanocyte stimulating hormone; CA, Centella asiatica; GCA, Giant CA.

asiaticoside. These findings provide insight into the potential active components responsible for the superior skin-whitening effects of the GCA extract observed in the aforementioned experiments.

Inhibitory effects of madecassoside and asiaticoside on melanin production and their binding to MC1R. Treatment with asiaticoside and madecassoside significantly reduced melanin production (Fig. 4A). Asiaticoside showed a more potent inhibitory effect than that of madecassoside. Conversely, madecassic acid and asiatic acid had minimal effects on inhibiting melanin production, which may explain GCA's superior efficacy in suppressing melanin production considering the higher content of asiaticoside and madecassoside in GCA than in CA (Fig. 3B). Pull-down assay results confirmed that asiaticoside and madecassoside directly bound to MC1R (Fig. 4B and C). Interestingly, increasing concentrations of α-MSH led to decreased binding of asiaticoside and madecassoside to MC1R. This finding suggests that asiaticoside and madecassoside compete with α-MSH for binding to MC1R.

Molecular docking studies on the interaction between MC1R and two major triterpenoids. To further investigate the binding of asiaticoside or madecassoside to MC1R, molecular docking studies were performed using the human MC1R structure. Previous studies have suggested that the GLU94 of MC1R greatly influences ligand binding and receptor function (41). The present docking model results revealed that both asiaticoside and madecassoside bound to GLU94 of MC1R, with docking energies of -9.9 and -8.6 kcal/mol, respectively (Fig. 5A and B). By contrast, the docking energy of α-MSH

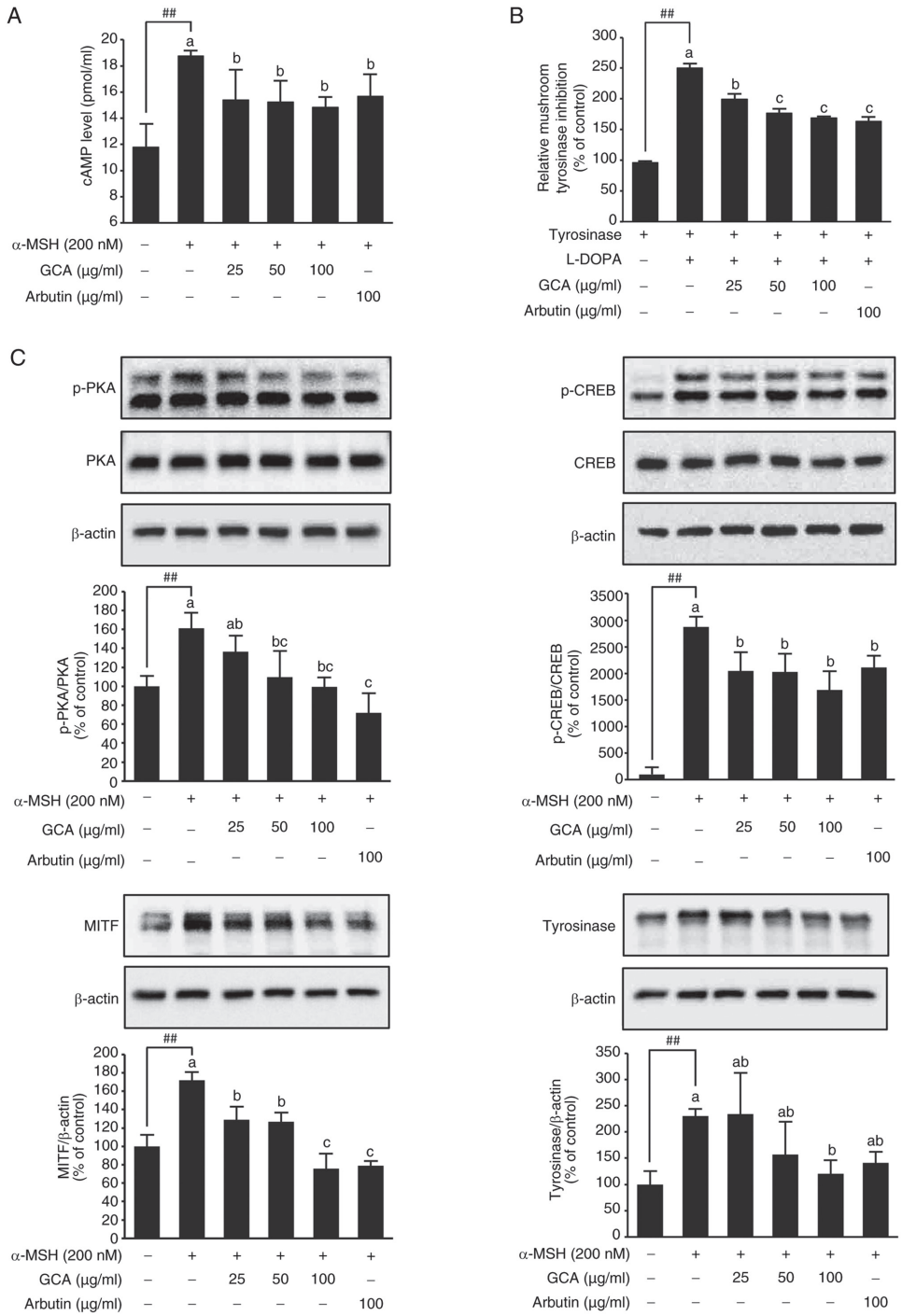

Figure 2. Inhibition of the melanogenesis-related signaling and tyrosinase activity by the GCA extract. (A) The GCA extract reduces cAMP levels, indicating its potent modulatory effect on cAMP-dependent pathways critical for melanogenesis. $^{\#\#}$P<0.01 between the control and α-MSH. Data are presented as mean values ± SD (n=3). Mean values with different letters indicate statistically significant differences among the treatment groups, including the α-MSH-induced group, as determined by one-way ANOVA followed by Tukey's HSD test (P<0.05). (B) Concentration-dependent inhibitory effect of the GCA extract and arbutin on mushroom tyrosinase activity. Significant differences were observed between the tyrosinase and tyrosinase group + L-DOPA group ($^{\#\#}$P<0.01). Moreover, the addition of GCA at concentrations of 25, 50 and 100 μg/ml and arbutin 100 μg/ml to the tyrosinase + L-DOPA group significantly reduced the relative mushroom tyrosinase activity compared with that in the tyrosinase + L-DOPA group, as determined by one-way ANOVA followed by Tukey's HSD test (P<0.05). (C) Effects of GCA extract on the expression and phosphorylation of PKA, CREB, MITF and tyrosinase in B16F10 cells. Protein expression levels were determined in cell lysates using specific antibodies by immunoblotting. β-actin was used as a loading control. Representative western blots from three independent experiments are shown (n=3). Significant differences between untreated control and α-MSH-induced group ($^{\#\#}$P<0.01). Mean values with different letters indicate statistically significant differences among the treatment groups, including the α-MSH-induced group, as determined by one-way ANOVA followed by Tukey's HSD test (P<0.05). α-MSH, α-melanocyte stimulating hormone; CA, *Centella asiatica*; GCA, Giant CA; PKA, cAMP-dependent protein kinase; CREB, cAMP response element-binding protein; MITF, microphthalmia-associated transcription factor.

was higher at -6.9 kcal/mol. These results suggested that asiaticoside and madecassoside may bind more strongly to MC1R than α-MSH, which is consistent with the findings from the pull-down assay (Fig. 4B and C). While the aforementioned Autodock results indicated that asiaticoside has higher potency than madecassoside, further analysis using

A

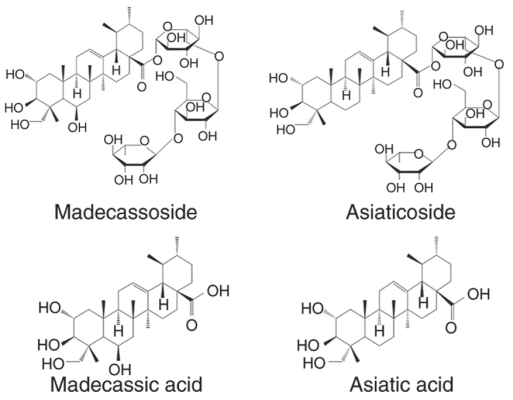

B

Major triterpenoids	GCA (mg/g)	CA (mg/g)
Madecassoside	10.43±0.05	2.53±0.01
Madecassic acid	4.97±0.01	15.51±0.05
Asiaticoside	1.65±0.01	0.95±0.01
Asiatic acid	4.03±0.02	12.84±0.06

Figure 3. Molecular structures of the major triterpenoids identified in the GCA and CA extracts. (A) The structures of madecassoside, asiaticoside, madecassic acid and asiatic acid are shown. (B) Quantitative analysis of these compounds in the GCA and CA extracts. The concentrations of madecassoside, madecassic acid, asiaticoside and asiatic acid in the GCA and CA extracts are presented in mg/g. CA, *Centella asiatica*; GCA, Giant CA.

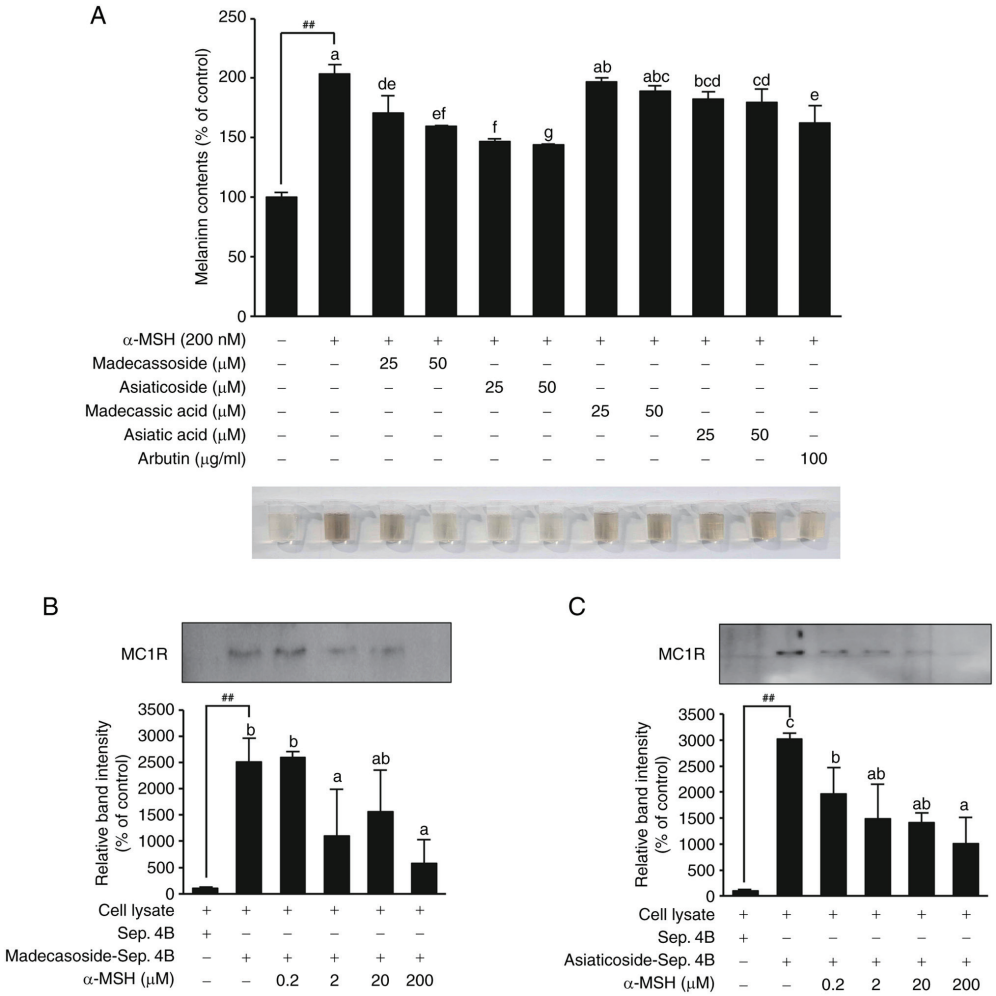

Figure 4. Inhibitory effects of madecassoside and asiaticoside on melanin synthesis and their direct binding to MC1R. (A) Inhibitory effects of madecassoside and asiaticoside on α-MSH-induced melanin production in B16F10 cells. Significant differences between the untreated control and α-MSH-induced group ($^{\#\#}$P<0.01). Mean values with different letters indicate statistically significant differences among the treatment groups, including the α-MSH-induced group, as determined by one-way ANOVA followed by Tukey's HSD test (P<0.05). (B and C) Confirmation of direct binding between (B) madecassoside, (C) asiaticoside and MC1R by pull-down assay. Sepharose 4B beads alone were used as a negative control. Sepharose 4B beads conjugated with madecassoside or asiaticoside were used to examine binding to MC1R. Competitive binding between madecassoside, asiaticoside and MC1R was assessed by treating with increasing concentrations of α-MSH. The significant differences between the Sepharose 4B beads only control (lane 1) and the madecassoside- or asiaticoside-conjugated beads (lane 2) confirmed the binding of madecassoside and asiaticoside to MC1R ($^{\#\#}$P<0.01). Evaluation of the competitive binding between α-MSH and madecassoside or asiaticoside showed significant differences in MC1R expression between the group without α-MSH treatment (lane 2) and the groups treated with increasing concentrations of α-MSH (0.2, 2, 20 and 200 μM; lanes 3-6). Mean values with different letters indicate statistically significant differences among the treatment groups, as determined by one-way ANOVA followed by Tukey's HSD test (P<0.05). Additionally, differences in MC1R expression at the same α-MSH concentration were evaluated to compare the extent of competitive binding with α-MSH between madecassoside and asiaticoside. α-MSH, α-melanocyte stimulating hormone; MC1R, melanocortin 1 receptor.

A

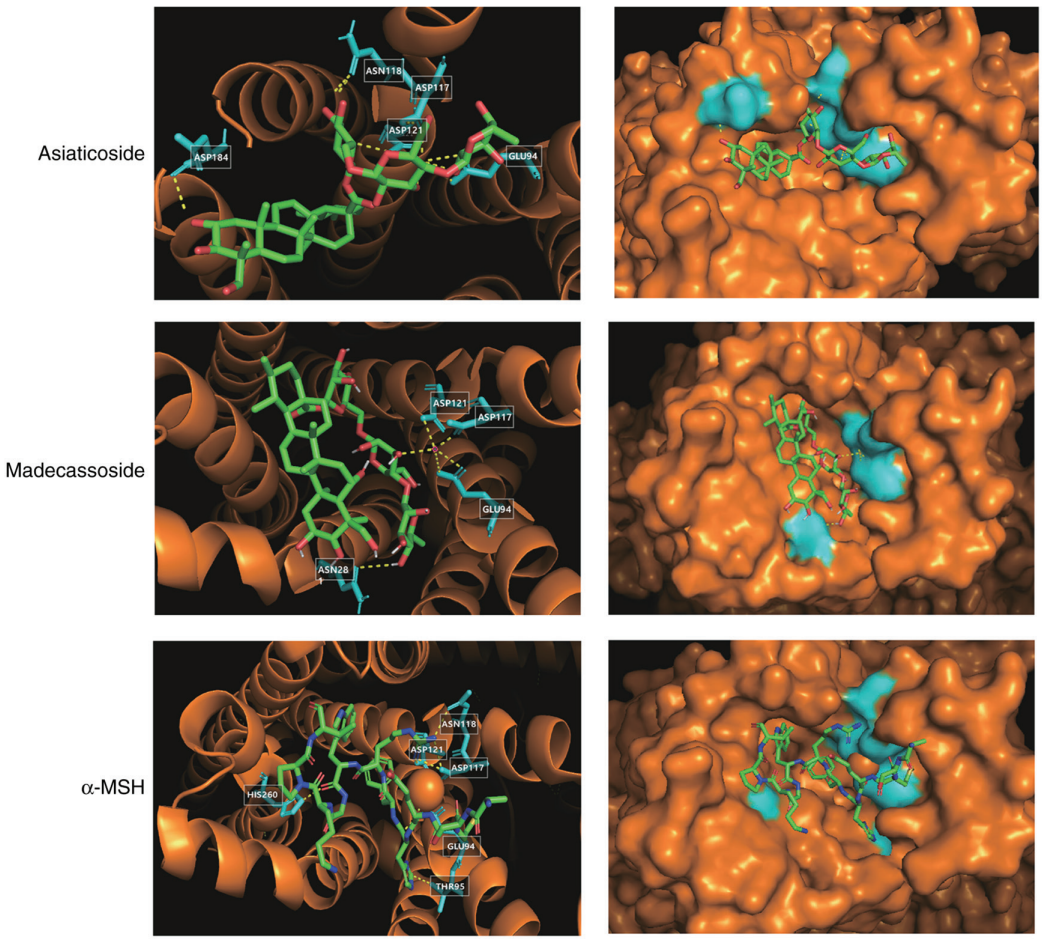

B

Rank	Compound	Docking energy (kcal/mol)	MolDock Score
1	Asiaticoside	–9.9	–224.697
2	Madecassoside	–8.6	–209.118
3	α-MSH	–6.9	–

Figure 5. Modeling study of MC1R binding to triterpenoid. (A) Binding of madecassoside and asiaticoside to the GLU94 of MC1R (blue stick: ligand; orange: MC1R, yellow dotted line: hydrogen bond). (B) Predicted binding energies of madecassoside, asiaticoside and α-MSH to MC1R. α-MSH, α-melanocyte stimulating hormone; MC1R, melanocortin 1 receptor.

MolDock confirmed this observation. The MolDock binding scores for asiaticoside were -224.697, which were higher than those for madecassoside, which scored -209.118. These results provide stronger evidence of the higher binding affinity of asiaticoside (Fig. 5B). However, due to the large molecular weight of α-MSH, it was not possible to obtain α-MSH MolDock results.

Inhibitory effect of the GCA extract on melanin synthesis in a 3D human skin-equivalent model. To further validate the anti-melanogenic effects of the GCA extract in a more physiologically relevant context, a 3D human skin-equivalent model (Neoderm®-ME) was used. This model incorporates human melanocytes and exhibits natural melanogenesis over time, closely mimicking human skin (1). Neoderm®-ME was treated with 25, 50 and 100 μg/ml GCA extract, 100 μg/ml CA extract, and arbutin as a positive control. After 7 days of treatment, the GCA extract at 100 μg/ml significantly reduced melanin content by 64% relative to that in the control, outperforming both the CA extract (30% reduction) and arbutin (Fig. 6A). The expression of tyrosinase, a critical enzyme in melanin synthesis, was also markedly decreased in the presence of the GCA extract, particularly at 100 μg/ml (Fig. 6B). This reduction in tyrosinase expression is associated with the observed decrease in melanin production (Fig. 6A). Furthermore, Fontana-Masson staining, which enables visualization of melanin in tissue sections, revealed a notable reduction in staining intensity in samples treated with the GCA extract (Fig. 6C), corroborating the quantitative data and tyrosinase expression patterns. Collectively, these findings demonstrated that the GCA extract effectively inhibits melanogenesis in a 3D human skin-equivalent model,

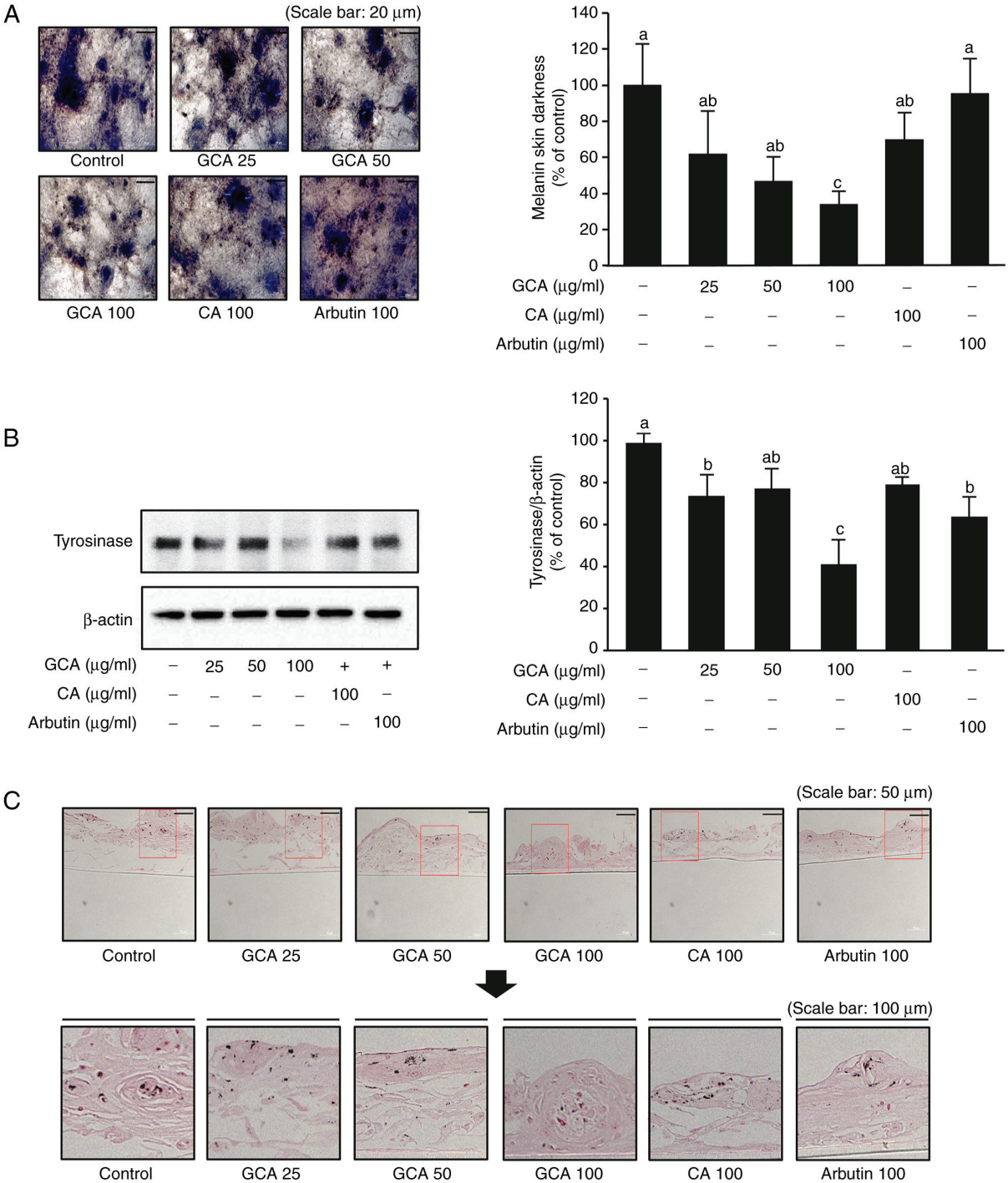

Figure 6. Inhibition of melanogenesis by the GCA extract in a 3D human skin-equivalent model. (A) Effects of the GCA extract on melanin synthesis and skin darkness in a 3D human skin-equivalent model. The scale bar indicates 20 μm. Data (n=3) are the mean values ± SEM. (B) The inhibitory effects of the GCA extract on tyrosinase protein expression were determined by western blotting. Protein expression levels were determined in cell lysates by use of specific antibodies and immunoblotting. β-actin was used as a loading control. Representative western blots from three independent experiments are shown (n=3). (C) Fontana-Masson staining images for visualizing melanin content in tissue sections. Upper panel: Images with scale bar indicating 50 μm. Lower panel: Magnified images of the areas highlighted in red boxes, with a scale bar indicating 100 μm. Mean values with different letters indicating statistically significant differences compared with the control group, as determined by one-way ANOVA followed by Tukey's HSD test (P<0.05). CA, *Centella asiatica*; GCA, Giant CA.

suppressing both melanin production and tyrosinase expression. These results, in conjunction with the molecular docking studies and binding assays, provide compelling evidence that the anti-melanogenic effects of the GCA extract were superior to those of the CA extract, highlighting its potential as a natural skin-whitening agent.

Discussion

The present study demonstrated that the GCA extract, derived from a new species of CA, exhibited efficacy for inhibiting α-MSH-induced melanin production superior to that of the traditional CA extract. The enhanced inhibitory effect of the

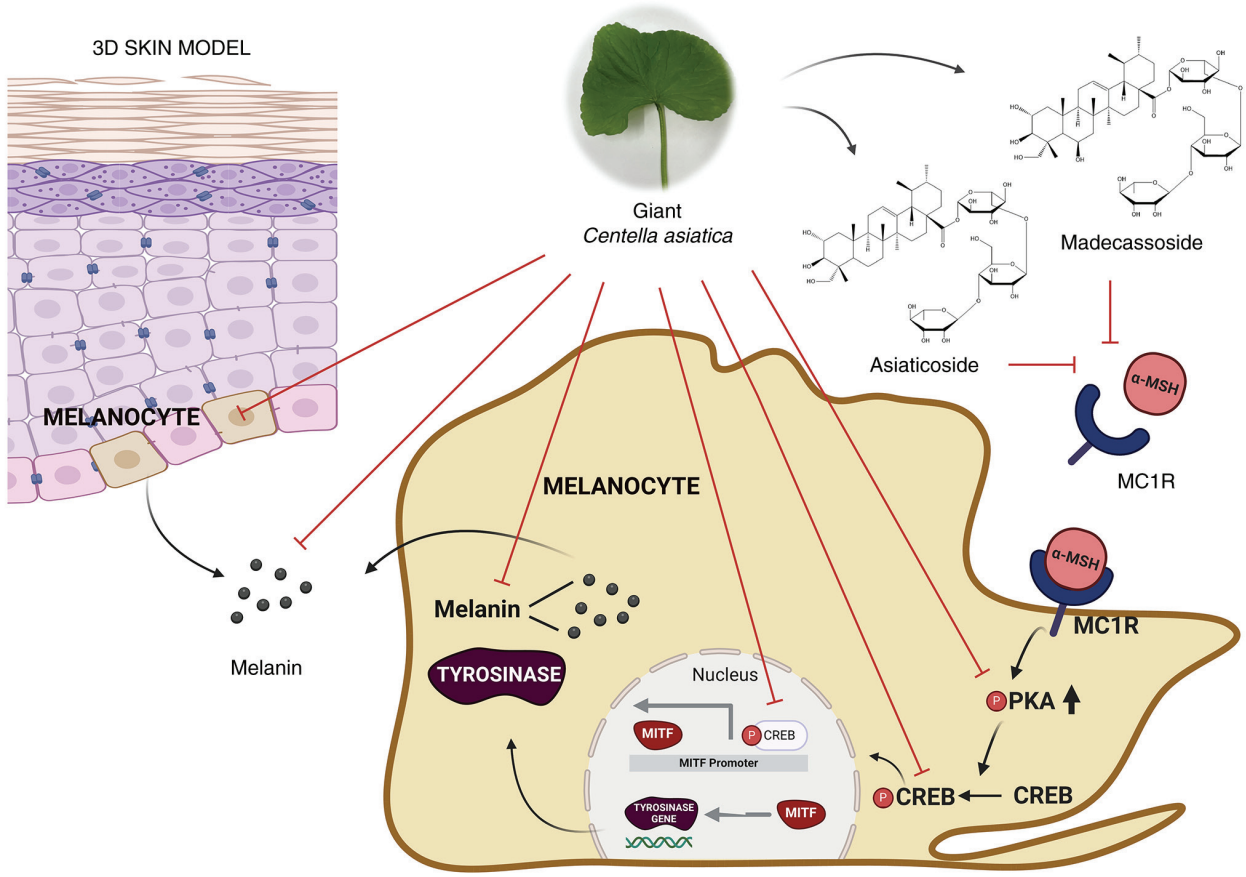

Figure 7. Schematic representation of the anti-melanogenesis effects of giant *Centella asiatica*. PKA, cAMP-dependent protein kinase; CREB, cAMP response element-binding protein; MC1R, melanocortin 1 receptor.

GCA extract on melanogenesis can be attributed to its higher content of key components, particularly madecassoside and asiaticoside. The results of the present study identified that melanin production was more effectively reduced by the GCA extract than by the CA extract at various concentrations. HPLC-MS/MS analysis revealed that the content of madecassoside and asiaticoside was significantly higher in the GCA extract than in the CA extract. These findings suggest that the higher concentrations of these active compounds in the GCA extract contributed to its enhanced inhibition of melanin production.

To further elucidate the mechanism of action, the interaction between the two major active compounds, madecassoside and asiaticoside, and MC1R, a key receptor in melanogenesis, were investigated. Molecular docking simulations revealed that both compounds bind to the GLU94 residue of MC1R, with binding affinities higher than that of α-MSH. Interestingly, despite their competitive binding to MC1R, madecassoside and asiaticoside did not promote melanin production, unlike α-MSH. This finding suggests that these compounds may act as antagonists of MC1R, inhibiting α-MSH-induced receptor activation and downstream signaling pathways leading to melanin synthesis. The potential antagonistic activity of madecassoside and asiaticoside on MC1R is reminiscent of the mechanism of action of agouti signaling protein (ASIP), a well-known endogenous antagonist of MC1R. ASIP competes with α-MSH for binding to MC1R and inhibits cAMP production, resulting in decreased melanin formation (42). The similar binding patterns and effects on melanin production observed with madecassoside and asiaticoside suggest that these compounds may function as MC1R antagonists, analogous to ASIP, but further studies are needed to confirm their effect on MC1R signaling and to elucidate the structural basis of their antagonistic activity. This consistency between computational predictions and experimental results further validates the reliability of molecular modeling approach in the present study.

From an industrial perspective, GCA extracts show significant potential for incorporation into various skincare products, particularly in the growing market for natural and plant-based cosmeceuticals. The use of water extraction methods in obtaining GCA extracts offers a notable advantage, making the production process more environmentally friendly and cost-effective compared with organic solvent extractions (43). Furthermore, GCA contains higher concentrations of active compounds, specifically madecassoside and asiaticoside, compared with traditional CA. The present study aimed to identify the most effective compounds for inhibiting melanogenesis, and madecassoside and asiaticoside were selected due to their high concentrations in GCA extract and their anti-melanogenic properties, which were confirmed through experimental data (Fig. 3B). This higher potency could allow for more effective formulations or the use of lower doses in skincare products. Additionally, the higher yield of GCA cultivation compared with traditional CA suggests a more efficient and economically viable production process (25). These factors combined could lead to more sustainable and cost-effective

production of skin-whitening ingredients, offering a promising alternative in the cosmetics and skincare industry. However, challenges such as maintaining compound stability in formulations, ensuring consistent extract quality, and scaling up production will need to be addressed in the product development process. Despite these challenges, the industrial potential of GCA extracts remains significant, presenting opportunities for innovation in natural skincare products.

While the current study provides strong evidence for the efficacy of GCA extracts in inhibiting melanogenesis, it is important to note that these findings are primarily based on *in vitro* and 3D skin model experiments. Future research directions could include exploring synergistic effects with other skin-whitening agents and investigating these compounds' potential to address additional skin concerns. Further *in vivo* studies and clinical trials are crucial to validate the efficacy and safety of GCA on human skin, fully elucidate its mechanisms of action, and optimize its application in skincare products. The promising results from the present study provide a strong foundation for future investigations and potential industrial applications in the field of dermatology and cosmetics.

In conclusion, the present study established the GCA extract to be a potent inhibitor of melanogenesis, with efficacy superior to that of traditional CA extract. The higher content of madecassoside and asiaticoside in GCA significantly contributed to its enhanced skin-whitening effects. Additionally, to the best of our knowledge, this is the first study to demonstrate that the two principal compounds, madecassoside and asiaticoside, bind to MC1R and contribute to the skin-whitening effect through their interaction with this receptor. The proposed mechanism of action for GCA's anti-melanogenic effects is summarized in Fig. 7. This discovery is of significant academic importance as it highlights the unique mechanism by which these compounds inhibit melanogenesis, thereby offering new insights into their potential applications in dermatological treatments. Further research, including clinical trials, is crucial to validate the efficacy of GCA on human skin whitening and fully elucidate its mechanisms of action.

Acknowledgements

Not applicable.

Funding

The present study was supported by BOBSNU Co. Ltd., ASK Company Co. Ltd., Brain Korea 21 Plus Program of the Department of Agricultural Biotechnology, Seoul National University and the Bio and Medical Technology Development Program of the National Research Foundation (NRF), funded by the Korean government (MSIT) (grant no. 2020M3H1A1073304). The present study was also supported by the NRF of Korea (NRF) grant funded by the Korea government (MSIT) (grant no. RS-2024-00333238).

Availability of data and materials

The data generated in the present study may be requested from the corresponding author.

Authors' contributions

JS, CJ, SL, HWP, DBS, DSY, TL, JHYP, CHL and KWL conceived and designed the experiments. JS, CJ, SO and WS performed the experiments. SL, HWP, DBS, DSY, CHL and KWL provided resources and funding. JS, TL, JHYP, CHL and KWL prepared and revised the manuscript. JS, CJ, HWP, DBS, DSY, TL, JHYP, CHL and KWL analyzed the data and supervised the project. JS, CJ, SO, SL, HWP, DBS, DSY, WS, JHYP, CHL and KWL confirm the authenticity of all the raw data. All authors read and approved the final version of the manuscript.

Ethics approval and consent to participate

Not applicable.

Patient consent for publication

Not applicable.

Competing interests

The authors declare that they have no competing interests.

Authors' information

JS, 0000-0001-9680-7068; CJ, 0009-0007-3198-868X; SO, 0009-0008-1909-8761; SL, 0000-0002-3057-3243; WS,0000-0002-0903-3701; TL, 0000-0001-6930-9565; JHYP, 0000-0002-5518-4279; CHL, 0000-0002-1907-4400; KWL, 0000-0001-6302-2432.

References

1. Shon YJ, Kim WC, Lee SH, Hong S, Kim SY, Park MH, Lee P, Lee J, Park KH, Lim W. and Lim TG: Antimelanogenic potential of brewer's spent grain extract through modulation of the MAPK/MITF axis. Sustain. Mater. Technol 38: e00721, 2023.
2. Hong S, Lee S, Sim WJ, Kim WC, Kim SY, Park MH, Lim W and Lim TG: Ultrasound-assisted pumpkin tendril extracts inhibits melanogenesis by suppressing the CREB/MITF signaling pathway in B16F10 melanoma cells, zebrafish, and a human skin model. J Funct Foods 109: 105813, 2023.
3. Ito S; IFPCS: The IFPCS presidential lecture: A chemist's view of melanogenesis. Pigment Cell Res 16: 230-236, 2003.
4. Videira IF, Moura DF and Magina S: Mechanisms regulating melanogenesis. An Bras Dermatol 88: 76-83, 2013.
5. Böhm M, Wolff I, Scholzen TE, Robinson SJ, Healy E, Luger TA, Schwarz T and Schwarz A: alpha-Melanocyte-stimulating hormone protects from ultraviolet radiation-induced apoptosis and DNA damage. J Biol Chem 280: 5795-5802, 2005.
6. García-Borrón JC, Abdel-Malek Z and Jiménez-Cervantes C: MC1R, the cAMP pathway, and the response to solar UV: Extending the horizon beyond pigmentation. Pigment Cell Melanoma Res 27: 699-720, 2014.
7. Dessinioti C, Antoniou C, Katsambas A and Stratigos AJ: Melanocortin 1 receptor variants: functional role and pigmentary associations. Photochem Photobiol 87: 978-987, 2011.
8. Park HY, Wu C, Yonemoto L, Murphy-Smith M, Wu H, Stachur CM and Gilchrest BA: MITF mediates cAMP-induced protein kinase C-beta expression in human melanocytes. Biochem J 395: 571-578, 2006.
9. Shin H, Hong SD, Roh E, Jung SH, Cho WJ, Park SH, Yoon DY, Ko SM, Hwang BY, Hong JT, *et al*: cAMP-dependent activation of protein kinase A as a therapeutic target of skin hyperpigmentation by diphenylmethylene hydrazinecarbothioamide. Br J Pharmacol 172: 3434-3445, 2015.

10. Zhang H, Kong Q, Wang J, Jiang Y and Hua H: Complex roles of cAMP-PKA-CREB signaling in cancer. Exp Hematol Oncol 9: 32, 2020.
11. Taylor SS, Kim C, Cheng CY, Brown SH, Wu J and Kannan N: Signaling through cAMP and cAMP-dependent protein kinase: Diverse strategies for drug design. Biochim Biophys Acta 1784: 16-26, 2008.
12. Ahmed MB, Alghamdi AAA, Islam SU, Lee JS and Lee YS: cAMP Signaling in Cancer: A PKA-CREB and EPAC-Centric Approach. Cells 11: 2020, 2022.
13. Hartman ML and Czyz M: MITF in melanoma: Mechanisms behind its expression and activity. Cell Mol Life Sci 72: 1249-1260, 2015.
14. Gelmi MC, Houtzagers LE, Strub T, Krossa I and Jager MJ: Mitf in normal melanocytes, cutaneous and uveal melanoma: A delicate balance. Int J Mol Sci 23: 6001, 2022.
15. Pillaiyar T, Manickam M and Namasivayam V: Skin whitening agents: Medicinal chemistry perspective of tyrosinase inhibitors. J Enzyme Inhib Med Chem 32: 403-425, 2017.
16. Mohania D, Chandel S, Kumar P, Verma V, Digvijay K, Tripathi D, Choudhury K, Mitten SK and Shah D: Ultraviolet Radiations: Skin defense-damage mechanism. Adv Exp Med Biol 996: 71-87, 2017.
17. Zamudio Díaz DF, Busch L, Kröger M, Klein AL, Lohan SB, Mewes KR, Vierkotten L, Witzel C, Rohn S and Meinke MC: Significance of melanin distribution in the epidermis for the protective effect against UV light. Sci Rep 14: 3488, 2024.
18. Torbati FA, Ramezani M, Dehghan R, Amiri MS, Moghadam AT, Shakour N, Elyasi S, Sahebkar A and Emami SA: Ethnobotany, phytochemistry and pharmacological features of *Centella asiatica*: A comprehensive review. Adv Exp Med Biol 1308: 451-499, 2021.
19. Bylka W, Znajdek-Awiżeń P, Studzińska-Sroka E and Brzezińska M: *Centella asiatica* in cosmetology. Postepy Dermatol Alergol 30: 46-49, 2013.
20. Sun B, Wu L, Wu Y, Zhang C, Qin L, Hayashi M, Kudo M, Gao M and Liu T: Therapeutic potential of *Centella asiatica* and its triterpenes: A review. Front Pharmacol 11: 568032, 2020.
21. Park KS: Pharmacological effects of *Centella asiatica* on skin diseases: Evidence and possible mechanisms. Evid Based Complement Alternat Med 2021: 5462633, 2021.
22. Idana F, Putra WAAG and Winarti NW: *Centella asiatica* extract cream inhibited microphthalmia-associated transcription factor (MITF) expression and prevented melanin amount increase in Guinea pig skin exposed to ultraviolet-B. Neurologico Spinale Medico Chirurgico 5: 27-31, 2022.
23. Bylka W, Znajdek-Awiżeń P, Studzińska-Sroka E, Dańczak-Pazdrowska A and Brzezińska M: *Centella asiatica* in dermatology: An overview. Phytother Res 28: 1117-1124, 2014.
24. Gohil KJ, Patel JA and Gajjar AK: Pharmacological review on *Centella asiatica*: A potential herbal cure-all. Indian J Pharm Sci 72: 546-556, 2010.
25. Oh S, Park S, Lee S, Park Y, Jang KI, Yu KW, Kim D and Shin H: Comparison of growth characteristics and physiological activity of two *Centella asiatica* cultivars in greenhouse soil culture. J Bio-Environ Control 30: 351-358, 2021.
26. Park H, Seo JW, Lee TK, Kim JH, Kim JE, Lim TG, Park JHY, Huh CS, Yang H and Lee KW: Ethanol extract of Yak-Kong fermented by lactic acid bacteria from a Korean infant markedly reduces matrix metallopreteinase-1 expression induced by solar ultraviolet irradiation in human keratinocytes and a 3D skin model. Antioxidants (Basel) 10: 291, 2021.
27. Valdés-Tresanco MS, Valdés-Tresanco ME, Valiente PA and Moreno E: AMDock: A versatile graphical tool for assisting molecular docking with Autodock Vina and Autodock4. Biol Direct 15: 12, 2020.
28. Kim JH, Lee JE, Kim T, Yeom MH, Park JS, di Luccio E, Chen H, Dong Z, Lee KW and Kang NJ: 7, 3', 4'-trihydroxyisoflavone, a metabolite of the soy isoflavone daidzein, suppresses α-melanocyte-stimulating hormone-induced melanogenesis by targeting melanocortin 1 receptor. Front Mol Biosci 7: 577284, 2020.
29. Javed A, Alam MB, Naznin M, Ahmad R, Lee CH, Kim S and Lee SH: RSM-and ANN-based multifrequency ultrasonic extraction of polyphenol-rich *Sargassum horneri* extracts exerting antioxidative activity via the regulation of MAPK/Nrf2/HO-1 machinery. Antioxidants (Basel) 13: 690, 2024.
30. Nam G, An SK, Park IC, Bae S and Lee JH: Daphnetin inhibits α-MSH-induced melanogenesis via PKA and ERK signaling pathways in B16F10 melanoma cells. Biosci Biotechnol Biochem 86: 596-609, 2022.
31. Yoon Y, Bae S, Kim TJ, An S and Lee JH: Nodakenin inhibits melanogenesis Via the ERK/MSK1 Signaling Pathway. Pharmazie 78: 6-12, 2023.
32. Bahraman AG, Jamshidzadeh A, Keshavarzi M, Arabnezhad MR, Mohammadi H and Mohammadi-Bardbori A: α-Melanocyte-stimulating hormone triggers melanogenesis via activation of the aryl hydrocarbon receptor pathway in B16F10 mouse melanoma cells. Int J Toxicol 40: 153-160, 2021.
33. Seo GY, Ha Y, Park AH, Kwon OW and Kim YJ: Leathesia difformis extract inhibits α-MSH-induced melanogenesis in B16F10 cells via down-regulation of CREB signaling pathway. Int J Mol Sci 20: 536, 2019.
34. Kim DH, Shin DW and Lim BO: Fermented *Aronia melanocarpa* inhibits melanogenesis through dual mechanisms of the PI3K/AKT/GSK-3β and PKA/CREB pathways. Molecules 28: 2981, 2023.
35. Kim MJ, Mohamed EA, Kim DS, Park MJ, Ahn BJ, Jeung EB and An BS: Inhibitory effects and underlying mechanisms of Artemisia capillaris essential oil on melanogenesis in the B16F10 cell line. Mol Med Rep 25: 113, 2022.
36. Wu PY, You YJ, Liu YJ, Hou CW, Wu CS, Wen KC, Lin CY and Chiang HM: Sesamol inhibited melanogenesis by regulating melanin-related signal transduction in B16F10 cells. Int J Mol Sci 19: 1108, 2018.
37. Lim YJ, Lee EH, Kang TH, Ha SK, Oh MS, Kim SM, Yoon TJ, Kang C, Park JH and Kim SY: Inhibitory effects of arbutin on melanin biosynthesis of alpha-melanocyte stimulating hormone-induced hyperpigmentation in cultured brownish guinea pig skin tissues. Arch Pharm Res 32: 367-373, 2009.
38. Otręba M, Rok J, Buszman E and Wrześniok D: Regulation of melanogenesis: the role of cAMP and MITF. Postepy Hig Med Dosw (Online) 66: 33-40, 2012 (In Polish).
39. Kwon KJ, Bae S, Kim K, An IS, Ahn KJ, An S and Cha HJ: Asiaticoside, a component of *Centella asiatica*, inhibits melanogenesis in B16F10 mouse melanoma. Mol Med Rep 10: 503-507, 2014.
40. Jung E, Lee JA, Shin S, Roh KB, Kim JH and Park D: Madecassoside inhibits melanin synthesis by blocking ultraviolet-induced inflammation. Molecules 18: 15724-15736, 2013.
41. Prusis P, Schiöth HB, Muceniece R, Herzyk P, Afshar M, Hubbard RE and Wikberg JE: Modeling of the three-dimensional structure of the human melanocortin 1 receptor, using an automated method and docking of a rigid cyclic melanocyte-stimulating hormone core peptide. J Mol Graph Model 15: 307-317. 334, 1997.
42. Yang CW, Ran JS, Yu CL, Qiu MH, Zhang ZR, Du HR, Li QY, Xiong X, Song XY, Xia B, *et al*: Polymorphism in MC1R, TYR and ASIP genes in different colored feather chickens. 3 Biotech 9: 203, 2019.
43. Gallina L, Cravotto C, Capaldi G, Grillo G and Cravotto G: Plant extraction in water: Towards highly efficient industrial applications. Processes 10: 2233, 2022.